Pulsed Eddy Current Probe Development to Detect Inner Layer Cracks near Ferrous Fasteners Using COMSOL Modeling Software

Vijay K. Babbar*, Paul P. Whalen, and Thomas W. Krause
Royal Military College of Canada
*Corresponding author: Department of Physics, Royal Military College of Canada, Kingston, Ontario, K7K 7B4. Vijay.Babbar@rmc.ca

Abstract: Pulsed eddy current technology is being developed to detect inner layer defects in multilayered conductive structures. Earlier work successfully employed COMSOL Multiphysics finite element modeling software to develop and optimize a probe with coaxially coupled driving and pickup coils. Although the probe could detect defects underneath a 3.6 mm thick aluminum plate, it was not effective in detecting inner layer cracks that originated at a ferrous fastener. The present work describes modeling of a new probe design, comprising two pickup coils, connected in differential mode, placed outside a central driver. Modeled differential signals from a simulated crack at multiple depths are presented. The signal decreases with increasing crack depth, but the probe can potentially detect a 4.8 mm deep crack underneath aluminum plate. The software was also useful in visualizing diffusion of magnetic flux through the ferrous fastener and its interaction with the surrounding defect region, which helped optimize the probe design.

Keywords: Nondestructive testing, pulsed eddy current, transient eddy current, electromagnetic modeling, transient electromagnetic fields.

1. Introduction

Non-destructive pulsed eddy current (PEC) testing is an emerging technology that is being developed for investigation of multilayered aircraft wing structures where fatigue induced crack growth may originate near ferrous fasteners in the inner layers [1-6]. Locations of such hidden defects are not normally detectable by conventional eddy current or ultrasonic methods. The application of conventional eddy current techniques is limited by very small depths of penetration into the conducting structure. Defect detection becomes even more difficult in the presence of a ferrous fastener. Also, ultrasonic techniques do not work well with multilayer specimens due to strong reflections from interlayer boundaries. PEC for nondestructive testing has been successfully modeled using finite element (FE) methods [7-11] and therefore has the potential to aid in designing new probes for detection and sizing of cracks in these situations.

The present work is an extension of earlier work [10] that successfully employed COMSOL Multiphysics FE modeling software to develop and optimize a reflection-type probe where the driving and pickup coils were coupled coaxially. The probe could detect defects underneath a 3.6 mm thick aluminum plate and there was good agreement with experiment. However, it was not very effective at detecting inner layer cracks that originated at a ferrous fastener, as typically found in airplane wing structures. This necessitated the development of a different probe design.

The present work uses FE modeling to generate three-dimensional models of a new central-driver-differential-pickup (CDDP) probe, which consists of two differentially-coupled pickup coils located at 180° on either side of the central driver. The models employ a square wave to excite a driving coil and produce magnetic flux that diffuses through a ferrous fastener into the multilayered aluminum structure to induce eddy currents in the inner layers near the crack location [12, 13]. The magnetic flux generated by the induced currents is captured by the pickup coils to generate a differential pickup signal. A number of FE models covering a range of crack depths from 1.6 to 4.8 mm in steps of 0.8 mm in the presence of a ferrous fastener have been developed and the variations in position and amplitude of the differential peak signal are presented. The work also includes investigation of the experimental differential signal from an identical CDDP probe configuration over multilayer aluminum structures. A comparison of modeling and experimental results shows a good agreement.

2. Experimental Work

The circuit diagram of the transmit/receive probe used for experimental work as well as FE modeling is shown in Fig. 1. The primary circuit consists of a driver of resistance R_{PC} connected in series with a source of emf ε and internal resistance R_{IN} of 53 Ω. The driver current is determined by connecting an additional series resistance R_{PV} of 2 Ω and measuring the voltage across it. The secondary circuit contains a pickup coil of resistance R_{SC} that is positioned outside the driver and connected across an external load of 51 Ω. The coil dimensions and other circuit parameters are given in Table 1.

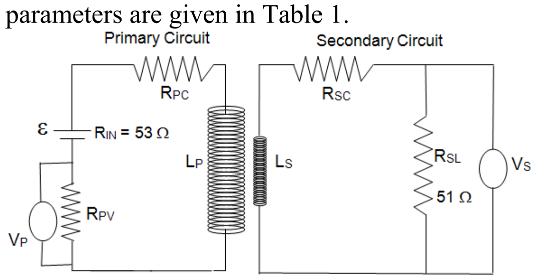

Figure 1. Circuit diagram of the probe configuration used for experiment as well as finite element modeling.

Table 1: CDDP Probe Specifications

	Driver	Pickup Coil	Driver Ferrite Core	Pickup Ferrite Core
Length, mm	20.0	1.0	40.0	10.0
Outer Dia, mm	10.0	4.0	8.0	1.0
Inner Dia, mm	8.5	1.0	-	-
Turns	1000	400	-	-
Gauge	38	44	-	-
Resistance, Ω	56.6	29.8	-	-
Inductance, mH	29.7	-	-	-
Lift-Off, mm	0.23	0.23	-	-
Permeability,	-	-	2300	48
Conductivity, S/m	-	-	0.5	0.5

Figures 2 and 3 show the actual probe configuration used to investigate defects in multilayer conducting samples in the presence of ferrous fasteners. It is a novel driver- pickup configuration, termed a Central Driver Differential Pickup probe [14, 15], which uses two pickup coils positioned equidistant from the central driver in a 180° configuration, as depicted in Fig. 3. The probe can also be used in a 90° configuration (not investigated in this work). The ferrous fastener passing through the plates channels the magnetic flux of the driver and facilitates generation of eddy currents at greater depths within the sample. The secondary magnetic field produced by these eddy currents is partly coupled to the pickup coil and produces an output signal.

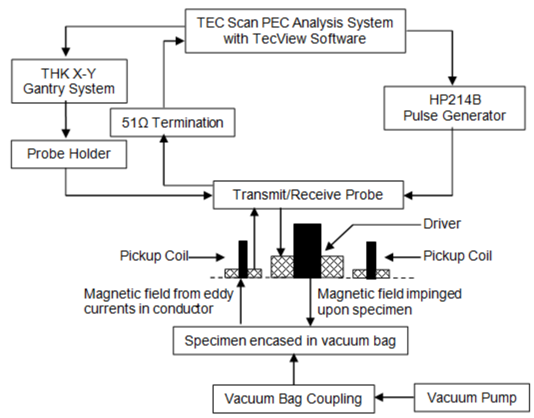

Figure 2. Block diagram of the experimental set-up used for the scanning system.

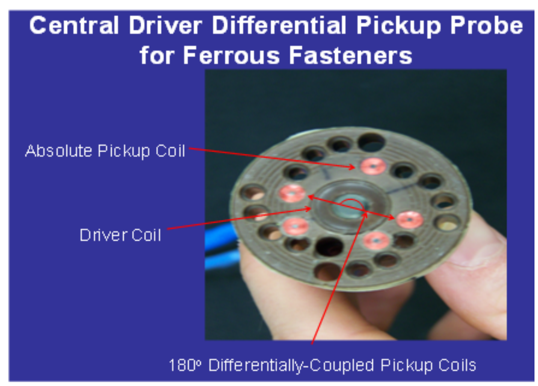

Figure 3. A hybrid CDDP probe showing the 180° differentially-coupled pickup coils modeled in this work.

3. Finite Element Modeling

The FE modeling was done using COMSOL Multiphysics 4.3 software. The detailed probe specifications used in the model are given in Table 1. The probe lift-off is 0.23 mm, which is the same as in the experiment. The two-fold symmetry in the model geometry was utilized to produce a half-model instead of a full-model in order to save computer resources and reduce computation time. For the same reason, sample plates of reduced size and circular geometry (diameter ~ 50 mm) were used. The 'Numeric' type driving and pickup coils were modeled.

A solved 3D half-model of a CDDP probe on a sample of aluminum plates is shown in Fig. 4. The sample consists of an upper plate of thickness 1.6 mm, a middle plate of thickness 2.0 mm and a lower plate of thickness 0.4 mm. Since the modeled plates have no air gap between them, the stack of plates can be assumed to be a continuum in order to reduce the model's memory requirements. Therefore, the sample is actually a plate of thickness 4.0 mm having a crack at the bottom surface. The vacuum bag used in the experiment minimizes air gaps between the plates, thus simulating the conditions of a continuum. A ferrous fastener bolt of length 13.8 mm and diameter 4.74 mm at the tail end passes through the plate. The through-crack in a 0.4 mm thick plate originates from the fastener hole and is located on the right side of the fastener at a depth of 4.0 mm. The crack has a length and width of 9.5 mm and 0.5 mm respectively as in the experiment. The mesh of a typical model constitutes about 200,000 mesh elements and 35,000 boundary elements. The software has a built-in step function to generate an almost square voltage pulse similar to the one produced by the experimental pulse generator [15]. The step function has a transition zone of 5×10^{-7} s. The total time varies from 0 to 5.00×10^{-3} s in steps of 5×10^{-6} s. A direct linear solver (MUMPS) is used to solve the model in the transient analysis mode.

To ascertain the validity of the FE modeling, a typical FE model with no sample or pickup coil was built and solved to obtain the driver air signal, which was compared with the corresponding signal from the experiment. The CDDP probe used in the experiment had five pickup coils around the driver. It was observed that the driver signal was influenced by their presence; hence a comparison of the air signal with sample and all pickup coils removed was made. The driver air signals from both experiment and FE modeling are shown in Fig. 5, which indicates excellent agreement between the two considering uncertainties in the experimental parameters.

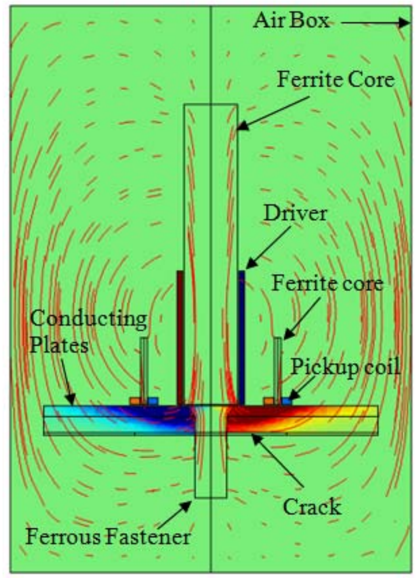

Figure 4. Front view of a solved 3D finite element half-model simulating the x component of the current density for the CDDP probe used in the experiment.

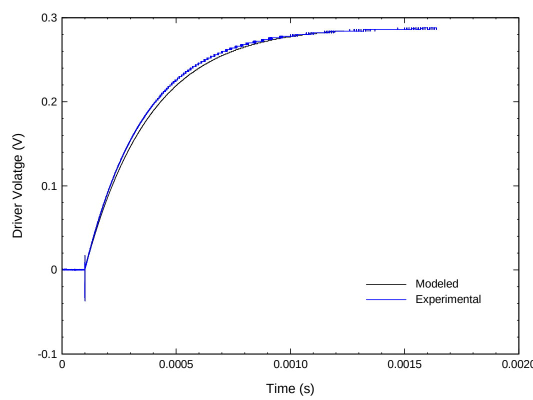

Figure 5. Comparison of driver air signal across 2 Ω resistor from experiment and FE modeling.

4. Results

4.1 Absolute and Differential Pickup Signals

Figure 6 shows a solved 3D model for the 4.0 mm crack depth showing distribution of magnetic flux through various components. The magnetic flux produced by the driver current is drawn into the structure by the ferrous fastener to generate induced currents in the conducting plates, which diffuse laterally with time and interact with the crack present on the underside of the aluminum plate. The secondary magnetic flux generated by these induced currents is sensed by the pickup coil to produce an output signal which is proportional to the induced current density within the plates.

The absolute defect and reference signals produced by the pickup coils match very closely with each other (Fig. 7) and, as such, reveal little information about the defect. The corresponding differential signal, although weak, can provide useful information about the severity and location of the defect. It typically consists of two peaks of opposite polarity—a very high initial peak followed by a shallow secondary peak of inverse polarity (Fig. 8). The first peak occurs due to direct interaction of the driver and sample with the two pickup coils in accordance with Lenz's law; it is only the second peak that carries information about the defects at depth, in particular those which are present within the inner layers.

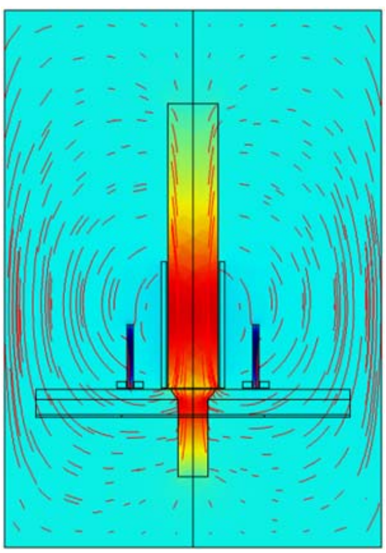

Figure 6. A solved 3D model showing flux penetration through the ferrous fastener.

4.2 Variation of differential pickup signal with crack depth

The variation of modeled differential pickup signal for a range of crack depths from 1.6 mm to 4.8 mm is shown in Fig. 9. The results are split into two depth regimes for clarity. A comparison of results reveals two types of variations—decrease in amplitude of the differential signal, and shifting of the signal peak to later times with increase in depth of crack and thickness of stack of plates. The decrease in amplitude and shifting of peak to later times are plotted separately in Figs. 10 and 11, respectively, along with experimental results for comparison.

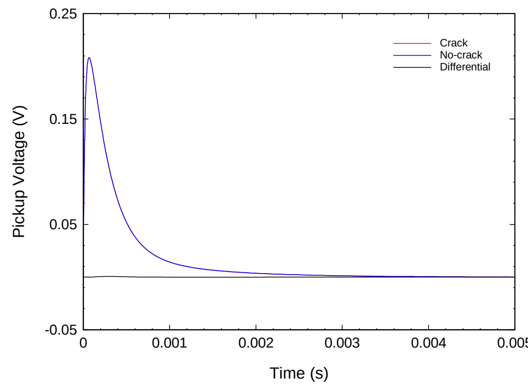

Figure 7. Modeled pickup coil signals from a 3.2 mm deep crack—absolute crack signal, absolute 'no-crack' signal, and differential signal.

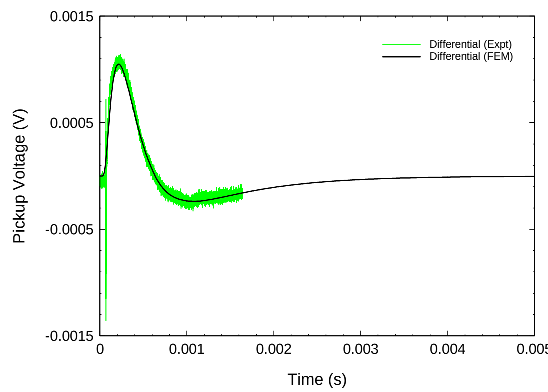

Figure 8. Magnified view of the differential pickup signal shown in Fig. 7. The corresponding experimental signal is also shown for comparison.

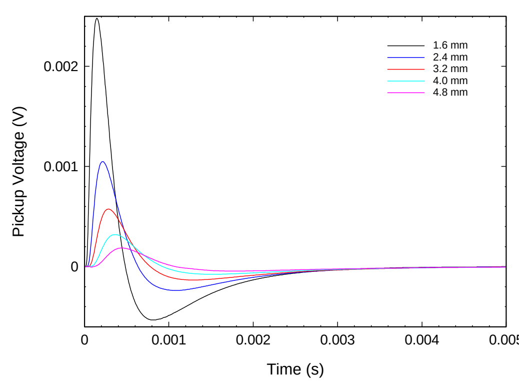

Figure 9: Differential pickup signal from crack depths of 1.6 to 4.8 mm.

As shown in Fig. 10, the peak amplitude varies non-linearly with change in crack depth. It decreases rapidly for shallower depths and slowly at greater depths. The models succeeded in predicting distinct, albeit weak, signals up to a depth of 5 mm for a crack of current dimensions, especially at a low noise level. The increase in time-to-peak with crack depth (Fig. 11) is almost linear and corresponds to a velocity of about 3.5 m/s of the second peak position, which represents the speed of flux diffusion through the structure and its reflection back to the pickup coil. This behavior may be described as that of a diffusion wave [12, 15].

The modeled results are in reasonably good agreement with experimental results as indicated by the close proximity of the experimental points to the modeled results. The mismatch of some of the experimental points is likely the result of variation in magnetic coupling between driver and ferrous fastener during the measurements.

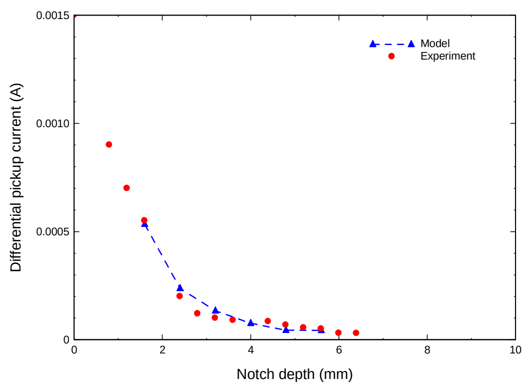

Figure 10: Variation of modeled and experimental differential pickup signal with crack depth.

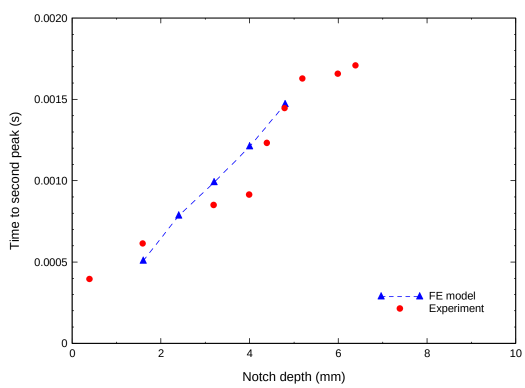

Figure 11: Variation of position of differential signal peak with crack depth.

5. Interpretation of Results

The differential response of the two pick-up coils, one mounted over the crack region and second on the no-crack region, may be considered in terms of differences in induced transient response of eddy currents within the conductor. The currents that are induced to expel the dynamic electric and magnetic fields according to Lenz's law in the aluminum around the hole [12, 16] arise, first, near the surface due to the applied field and, second, at greater depths due to the flux that is carried down through the layers of aluminum by the ferrous fastener at later times [12]. These induced currents will be forced around the crack, both over and further out into the aluminum, in comparison with the side without a crack, creating a differential field interaction between the two pick-up coils. With increasing depth of the crack, differences in field and induced current densities become weaker and the differential signal amplitude response is reduced. Reduction in amplitude response with increasing depth may be viewed as a result of attenuation of the electromagnetic field with longer travel time through the thickness of the plate stack above the crack.

6. Conclusions

The transient response of a probe with differentially connected pick-up coils mounted on either side of a driving coil was modeled using COMSOL Multiphysics modeling software. The probe was driven by a square pulse in order to generate transient eddy currents in a multilayered aluminum structure in the presence of a ferrous fastener. The finite element modeling was successful in simulating the transient response of the probe to a crack, which emanated from the fastener hole at the bottom of a stack of plates. The amplitude of the differential pickup signal was found to decrease non-linearly with increase in crack depth. The time-to-peak of the differential signal increased linearly with crack depth up to the maximum modeled depth of 4.8 mm. The variations of peak amplitude and peak position as a function of time are in good agreement with the experimental observations. These observations indicate that FE modeling can be used to test new probe designs and predict probe response to cracks in the vicinity of ferrous fasteners.

7. References

1. M. Gibbs, J. Campbell, Pulsed eddy current inspection of cracks under installed fasteners, *Materials Evaluation*, **49**, 51-59, (1991).
2. S. Giguere, J. M. S. Dubois, Finding corrosion independently of transducer lift-off, *Review of Progress in Quantitative Nondestructive Evaluation*, **19**, 449-456 (2000).
3. S. Giguere, B. A. Lepine, and J. M. S. Dubois, Pulsed eddy current technology: Characterizing material loss with gap and lift-off variations, *Review of Progress in Quantitative Nondestructive Evaluation*, **20**, 119-129 (2001).
4. S. Giguere, B. A. Lepine, and J. M. S. Dubois, Detection of cracks beneath rivet heads via pulsed eddy current technique, *Review of Progress in Quantitative Nondestructive Evaluation*, **21**, 1968-1974 (2002).
5. Y. A. Plotnikov, S. C. Nath and C.W. Rose, Defect characterization in multilayered conductive components with pulsed eddy current, *Review of Progress in Quantitative Nondestructive Evaluation*, **21**, 1976-1983 (2002).
6. T. W. Krause, C. Mandache, J. H. V. Lefebvre, Diffusion of pulsed eddy currents in thin conducting plates, *Review of Progress in Quantitative Nondestructive Evaluation*; **27**, 368-375 (2008).
7. U. Patel and D. Rodger, Finite element modelling of pulsed eddy currents for nondestructive testing, *IEEE Transactions on Magnetics*, **32**, 1593-1596 (1996).
8. H. Tsuboi, N. Seshima, I. Sebestyen, J. Pavo, S. Gyimothy, and A. Gasparics, Transient eddy current analysis of pulsed eddy current testing by finite element method, *IEEE Transactions on Magnetics*, **40**, 1330-1333 (2004).
9. V. K. Babbar, P. V. Kooten, T. J. Cadeau, and T. W. Krause, Finite element modeling of pulsed eddy current signals from conducting cylinders and plates, *35th Annual Review of Progress in Quantitative Nondestructive Evaluation, AIP Conf. Proc.*, **1096**, 311-318 (2009).
10. Vijay Babbar and Thomas Krause, Finite element modeling of transient eddy currents in multilayer aluminum structures, *Proceedings of the COMSOL Conference, Boston, USA* (2009).
11. V. K. Babbar, D. Harlley, and T. W. Krause, Finite element modeling of pulsed eddy current signals from aluminum plates having defects, *Review of Progress in Quantitative Nondestructive Evaluation*, **29A**, 337-344 (2010).
12. D. Desjardins, Analytical modeling for transient probe response in eddy current testing, *M.Sc. Thesis, Royal Military College of Canada* (2011).
13. D. R. Desjardins, G. Vallières, P. P. Whalen and T. W. Krause, Advances in transient (pulsed) eddy current for inspection of multi-layered aluminum structures in the presence of ferrous fasteners, *Review of Progress in Quantitative Nondestrutive Evaluation*, **31**, 440-407 (2012).
14. P. P. Whalen, V. Babbar, and T. W. Krause, Transient eddy current inspection in the presence of ferrous fasteners in multi-layered aluminum structures, *The 3rd International CANDU In-Service-Inspection and NDT in Canada 2010 Conference, Toronto, Ontario, Canada* (2010).
15. P. P. Whalen, Transient eddy current for the detection cracks in the vicinity of ferrous fasteners, *M.Sc. Thesis, Royal Military College of Canada* (2010).
16. H.C. Ohanian, On the approach to electro- and magneto-static equilibrium, *American Journal of Physics*, **51**, 1020-1022 (1983).

8. Acknowledgements

This work is supported by the Aerospace Research Advisory Committee, the Academic Research Program at the Royal Military College of Canada and Natural Sciences and Engineering Research Council of Canada.